# Uncertainty in DNP Target Data for E08-007

**D. Keller**[a]

[a] *University of Virginia,*
*U.VA. Dept. of Physics 382 McCormick rd Charlottesville, Va 22904-4714*
*E-mail:* dustin@jlab.org

ABSTRACT: A formal investigation into the uncertainty of polarized target data produced by Dynamic Nuclear Polarization is outlined. The polarization data taken during Jefferson Lab experiment E08-007 is used to obtain error estimates and to develop an algorithm to minimize uncertainty of the measurement of polarization in irradiated $NH_3$ targets. The target polarization and corresponding uncertainties for E08-007 are reported. For production data the uncertainties are less than or equal to $\Delta P/P = 3.28\%$.

## Contents



## 1. Introduction

The interest of the Jefferson Lab Hall A experiment E08-007 was to study the proton elastic form factor ratio $\mu G_E/G_M$ in the range of $Q^2$ = 0.01-0.7 GeV$^2$. The goal was to improve the knowledge of the ratio at low $Q^2$, which, in combination with separate cross section data, should also allow significant improvements in knowledge of the individual form factors. In this low $Q^2$ range, substantial deviations of the ratio from unity have been observed, and data, along with many fits and calculations, continues to suggest that structures might be present in the individual form factors, and in the ratio. Beyond the intrinsic interest in the structure of the nucleon, improved form factor measurements also have implications for deeply virtual Compton scattering, for determinations of the proton Zemach radius, and for parity violation experiments [1]. The data from experiment E08-007 can make well defined contributions to the building of our fundamental understanding. It is necessary to obtain high quality polarization data with low polarization uncertainty for the needed polarized target asymmetry measurements.

The experiment took place using Jefferson Lab's (JLAB) continuous electron beam in Hall A with energy between 1.1-2.2 GeV at beam current of approximately 100 nA. A system using a

refrigerator with sufficiently high cooling power to minimize the effects of microwave and beam heating on the polarization was built and installed into the experimental Hall. The target performance was optimized by the use of irradiated ammonia target material in a $^4$He evaporation refrigerator while using a magnetic field of 5 T, a large pumping system, and a high power EIO microwave tube operating at a frequency of $\sim$ 140 GHz.

Research in Nuclear physics with Dynamic Nuclear Polarized (DNP) targets has reached a state where understanding the uncertainty in polarization and being able to minimize that uncertainty is essential to the quality of physics and what can be reported about the polarization observables. Outlined here is a formal investigation into the polarization and uncertainty estimation of the polarized target data produced by DNP using the polarization data taken during Jefferson Lab experiment E08-007.

The polarized target data analysis took place off-line after the experiment was finished to ensure the quality of the polarization data. In addition to the resulting polarization data several instrumental errors, calibration uncertainties[1] and systematic uncertainties are laid out to study the full scope of target polarization error.

The notion of minimizing the uncertainty given multiple calibration runs is also explored. A $\chi^2$-minimization technique is used weighting each calibration by its combined total uncertainty.

## 2. Target Material

Experiment E08-007 required the fabrication of ammonia beads to serve as target material. This fabrication was done by the University of Virginia (UVA) polarized target lab [2]. Ammonia gas is condensed by sealing it in a teflon coated stainless steel under a liquid nitrogen ($LN_2$) bath at $\sim$77 K. This effectively freezes the ammonia into a solid. Once in the solid form, ammonia is crushed through mesh screens to form beads approximately 2 mm in diameter.

The target material for the experiment was irradiated to introduce paramagnetic radicals to optimize polarization performance. Studies indicate that it is advantageous to operate with high-temperature irradiated material [3, 4]. The preparation technique used was first developed and implemented with $NH_3$ in 1979 [5]. This irradiation process was performed creating an accumulated flux of high-intensity beam from a traveling-wave electron linac onto the ammonia. Protons are knocked-out from the $NH_3$ molecule to form $NH_2$ paramagnetic centers. The material was irradiated at the Medical Industrial Radiation Facility (MIRF) at the National Institute of Standards and Technology (NIST) in Gaithersburg, MD. The procedure involves using the MIRF 14 MeV electron beam at $\sim$10 $\mu$A to strike the material under a $\sim$87 K liquid argon (LA) bath. The irradiation required was approximately $10^{17} e^-/cm^2$ (120 min.).

Radiation damage to the target material happens when additional radicals in the target materials are created during the experiment. The Larmor frequency of the radiation-produced radicals deviates from that of $NH_3$ distorting the DNP process. As radical density increases, it affects the relaxation processes, shortening relaxation time and reducing nucleon polarization.

The polarization reduction can be almost completely recovered by heating or annealing the target material, not to exceed about 20° K below the devitrification temperature [6, 7]. The amount

[1] specific to JLAB/UVA Polarized target system

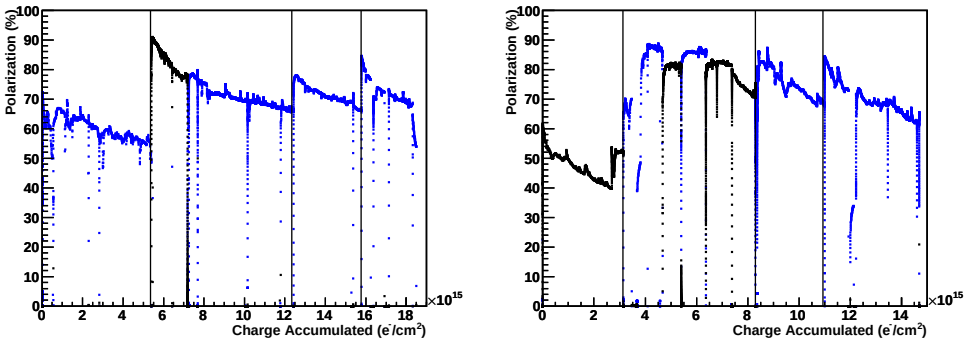


**Figure 1.** The top target cell is on the left with the bottom on the right. In each case the blue points are positively polarized and the black points are negative polarized.

of radiation damage sustained with the same beam flux increases after each anneal until the material must be changed. The radiation damage over the course of the experiment can be seen by studying polarization changes with respects to charge accumulated on the material from the JLAB Continuous Electron Beam Accelerator Facility (CEBAF) electron beam. The polarization as a function of charge accumulation is shown in Fig. 1. The same ammonia sample was used over the entire course of experiment E08-007. The charge accumulation is obtained using the Hall A beam current monitors (BCM) [8].

The material placed in the top target cell was irradiated at NIST for 140 minutes while the material placed in the bottom cell was irradiated for 120 minutes. The maximum absolute polarization during the commissioning runs were about 70% for the top cell and 60% for the bottom. This under-performance in the top cell is an indication that there may have been too many paramagnetic radicals present from the NIST irradiation. On the other hand the bottom cell performs a bit better after some dose has been put on it indicating that it may not have been irradiated enough. After the first anneal, at $5.4 \times 10^{15} e^{-}/cm^2$ ($3.1 \times 10^{15} e^{-}/cm^2$) for the top (bottom) cell in Fig. 1, the material performance improved reaching over 90% polarized. The first anneal had an average temperature of about 75 K for 15 minutes. Over the course of the experiment the anneals require a longer duration at a greater temperature but still less than 100° K. The other two anneals on the target materials are shown in Fig. 2. The points in charge accumulation that the anneals took place are indicated by the solid vertical lines seen in Fig 1.

The systematic effect of the reversal of the target polarization is checked by comparing the evolution of the polarization decay in Fig. 1. As seen in the top cell, Fig. 1 (left), the points from positive polarization match up with the points from negative polarization in the decay trend. In the bottom cup, Fig. 1 (right), this is less evident. The regions of flatness in the negative polarization are an indication that the microwave frequency was not set to optimize polarization over that time period. Under this conclusion no uncertainty is added based on positive and negative polarization differences.

The charge accumulation history is necessary to charge average the polarization over a data run to make the polarized target data available to use in physics analysis. This is discussed further

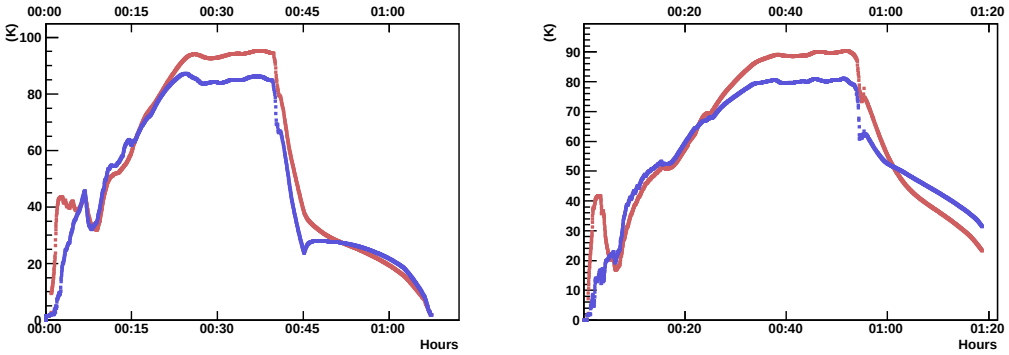


**Figure 2.** The temperature and duration for the second anneal (left) and third anneal (right). In each case the top cell is the red line and the bottom cell is the blue line.

in Section 7.

## 3. Polarized Target Data Analysis

The polarized target Nuclear Magnetic Resonance (NMR) and data acquisition included the software control system, the Rohde & Schwarz RF generator (R&S), the Q-meter enclosure, and the target inserts. The Q-meter enclosure contained two separate Liverpool Q-meters [9] and Yale gain cards which were used for different target cup cells during the experiment. The target material and NMR coil are held in polychlorotrifluorethyene (Kel-F) cells with the whole target insert cryogenically cooled to $\sim$ 1K.

The R&S produced a RF setup to drive a triangle wave of 1 kHz providing a sweep over frequency. The R&S responded to an external modulation sweeping linearly from 400 kHz below to 400 kHz above the Larmor frequency. The signal from the R&S was connected to the NMR coils within the target material. This connection was made with a $\lambda/2$ semi-rigid cable with a teflon dielectric. The signal from the Q-meter was passed through the Yale gain card before the signal was digitized. It is possible to enhance signal to noise information through the software control system by making multiple frequency sweeps and averaging the signals. A completion of the set number of sweeps resulted in a single target event with a time stamp. The averaged signal was integrated to obtain a NMR polarization area for that event. Each target event written contained all NMR system parameters and the target environment variables needed to calculate the final polarization. The on-line target data and conditions were analyzed over the experiments set of target events to return a final polarization and associated uncertainty for each run.

A Thermal Equilibrium measurement (TE) was used to find a proportionality relation to determine the enhance polarization under any thermal conditions given the area of the Q-curve signal. The TE natural polarization for a spin-1/2 particle is given by,

$$P_{TE} = \tanh\left(\frac{\mu B}{kT}\right), \tag{3.1}$$

coming from Curie's Law [10]. The dynamic polarization value is derived by comparing the enhanced signal $S_E$ integrated over the driving frequency $\omega$, with that of the (TE) signal:

$$P_E = G\frac{\int S_E(\omega)d\omega}{\int S_{TE}(\omega)d\omega}P_{TE} = GC_{TE}A_E, \tag{3.2}$$

and calibration constant defined as,

$$C_{TE} = \frac{P_{TE}}{A_{TE}}. \tag{3.3}$$

Where $P_E$ ($A_E$) is the polarization (area) of the enhanced signal, $P_{TE}$ ($A_{TE}$) is the polarization (area) from the thermal equilibrium measurement. The ratio of gains form the Yale card used during the thermal equilibrium measurement to the enhanced signal is represented as $G$. For experiment E08-007 the same gain setting was used for both but since the input voltage is slightly different at thermal equilibrium than for the enhance signal, $G$ can deviate from unity.

### 3.1 Yale Card Characteristics

The NMR signal from the Q-meter can be amplified by approximately 1, 20 or 50 times using the Yale card gains. There were two complete NMR circuits used in the experimental setup, one for the top target cup and the other for the bottom target cup. Both of the Yale cards were characterized to find a set of gains as a function of input voltage. These results enabled accurate calculation of the final polarization used in data analysis. These gain parameters were determined by sweeping the input voltage over a positive and negative range large enough to determine a clear trend. Figure 3 shows the trend for the Yale card used for the bottom target cup NMR configuration. The results shown are for the amplification of 1.

Measurements indicate that the Q-meter output voltage changes from TE signal of 3.2635 V to 3.3645 V at 90% enhanced polarization. These values include a DC offset of $\sim 3.2$ V. To obtain an accurate gain relation between the TE signal and the enhanced an experiment average production data polarization and resulting input voltage is divided by an averaged TE signal input voltage leading to $G = 0.999213$. This gain is used in the polarization calculation in Eq. 3.2. Because the gain is polarization dependent there is an uncertainty associated with using the average. This uncertainty is calculated to be $\sim 0.1\%$ in the overall polarization results.

### 3.2 NMR and Q-meter

The Q-meter uses the NMR coil as a sensing probe. This probe couples inductively with the magnetic moments of the nuclei in the material leading to a linear relation between the coil impedance and the complex magnetic susceptibility of the target material. The dispersion near resonance changes sign and has largest values near the Larmor frequency. The absorption, imaginary part, describes the spectral distribution of the precession frequencies of the spins near the NMR Larmor frequency and its integral is proportional to the nuclear polarization.

The Q-meter can be used outside experimental conditions to achieve relative polarization that can be measured to an accuracy of much less than 1%. During an experiment, environmental changes, NMR sampling non-uniformity and inhomogeneous radiation damage to the material all play an important role in adding uncertainties. An estimate of the latter can be obtained by studying

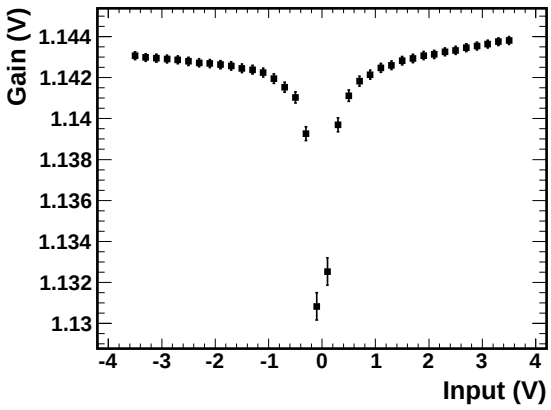


**Figure 3.** Yale card gains as a function of input voltage.

the difference in the beam flux on the material at different slow raster sizes between TE measurements.

Changes in Q-meter output voltage as a function of holding field have been measured to be smaller than $4.3 \times 10^{-4}$ over a range of 0 to 5 T. Under experimental operating conditions of the cryostat the Q-meter circuit tune does not shift and only small changes, $\Delta V/V < 1 \times 10^{-4}$, in the offset of the Q-meter output voltage are seen with respect to temperature.

There are known non-linearities in the Q-meter seen by measuring the power dissipated in the LCR circuit that can arise from changes in the ambient temperature of the Q-meter. The modulator output signal has a small temperature dependence that can be seen with constant input voltage and phase difference. This dependence was studied by measuring the Q-meter output voltage (or absolute polarization) in response to changes of the Q-meter circuit temperature. The relative deviation can change with respect to input signal, but not to a large degree. Several tests were performed at UVA to quantify this deviation. An example of polarized ammonia to a very stable 95.05% and the changes with respect to temperature of the Q-meter are shown in Figure 4. Tests were done on both of the Q-meters used in experiment E08-007. No changes are made in the polarized target analysis from these results but the uncertainty is considered. The experimental data indicated an average temperature of $21.2 \pm 1.2^{\circ}$ C, which at a polarization of 95% using a range of 2.4 C results in an uncertainty less than 0.54%. However, the uncertainty changes slightly depending on the polarization (input voltage) of the Q-meter.

The estimated uncertainty in absolute polarization from the Q-meter temperature dependence and NMR circuit issues mentioned is $\Delta P/P \sim 0.75\%$, which is an over estimation based on the effects seen over the course of the experiment.

### 3.3 NMR Signal Fitting and Integration

The TE measurements were carried out after thermalizing during the experiment, without beam and without microwaves. A baseline spectrum was taken by adjusting the magnetic field to be off-resonance. During the TE measurement, data is collected using the NMR baseline with the

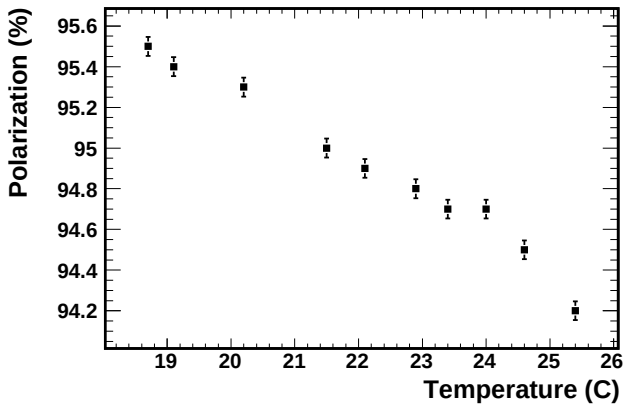


**Figure 4.** Polarization dependence on temperature using ammonia polarized to 95.05% at 21.5 °C.

TE signal spectrum. To compensate for drifts, the first and last 50 channels of the TE spectrum were used for a second order fit to the background which was then subtracted to give the final TE spectrum. The final TE spectrum is then integrated. Each of these proceeding steps can contribute uncertainty to the final TE area. The signal is of an unknown line shape and so it is integrated using a Riemann sum to obtain the signal area. An error estimate is achieved by combining the covariance information from the polynomial background fit and the error in the Riemann sum.

Enhanced signals were large enough that the uncertainty from the fit and Riemann sum became negligible ($\Delta P/P << 0.1\%$). In order to obtain an estimate in the TE Riemann sum, a Gaussian signal of average TE amplitude was generated on a standard baseline and the Riemann sum with background fit was used to obtain an area. It was found that the uncertainty is very much correlated with the slope of the polynomial fit where the signal sits. Accurate baseline and polynomial fit are critical for TE measurements. The final uncertainty in the TE area is found to be as much as 1.82%.

During the polarized target data analysis, the polynomial fit is checked to ensure a realistic background in relation to the signal location and to minimize fit errors using $\chi^2$-minimization. Only after the quality of the baselines are checked and the fit errors are minimized is the area of the TE and enhanced signal calculated. In most cases, a quality baseline is ascertained by checking all possible baselines and using the one closest to the TE measurement applied for that section of data. If the NMR tune is adjusted or fluctuates due to environmental conditions, the change will not be represented in a baseline taken earlier. One normally expects to use about 3000 sweeps when taking a baseline as to reduce statistical uncertainty. During TE data taking the number of sweeps is kept at 2000 or more to minimize the noise to signal.

## 4. Integrated Polarization Uncertainties

The total uncertainty from the calibration constant contains error in the TE area (see Section 3.3) as well as error in the TE polarization. Each separate component is propagated in accordance with Eq. 3.3. These uncertainties must be combined with the system's instrumental and systematic components. The latter is regulated through a TE fitting algorithm.

### 4.1 Thermal Equilibrium Polarization

For TE signals of protons, it is important to reduce the quality factor Q of the NMR circuit to minimize the modulation and the non-linearities. The TE signals for ammonia were taken at $\sim 1.5$ K. The temperature during the TE was necessarily very regular and only exhibits thermal fluctuations. Thermalization can take several hours depending on the material's previous state. The most accurate temperature of the material was measured with a liquid helium vapor pressure sensor connected to a Baratron 690A manometers. The standard accuracy of the Baratron manometer is about 0.12% with a $10^{-6}$ full scale resolution. The relation used to convert $^4$He liquid helium vapor pressure in Pascal to temperature in Kelvin is,

$$T = \sum_{i=0}^{9} a_i \left( \frac{\ln P - b}{c} \right)^i , \tag{4.1}$$

where the constants $a_i$, $b$, and $c$ are a set of parameters which depend on the state and temperature of the helium. A $^3$He bulb and manometer were used to check the temperature results. There is very good agreement between the $^4$He and $^3$He temperatures, which are equivalent within $\pm 12$ mK during the calibration runs. In addition changes from a Cernox thermistor in the target cell were correlated to changes in the temperature calculated from the $^4$He vapor pressure. Although the thermistor is not accurate enough to use in the TE measurement, it can help to understand the uncertainty in the temperature measurements. By studying the changes in temperature over time using the Cernox and the temperature from the $^4$He vapor pressure, a deviation was determined from the pressure probe being outside the material cell. The total instrumental uncertainty in using the $^4$He vapor pressure is $\Delta P_{inst} \sim 0.53\%$. This component of error is added in with the statistical and fit errors for each pressure measurement. The uncertainty in temperature as a function of pressure is expressed as,

$$\delta T = \sum_{i=1}^{8} a_i \left( \frac{\ln P - b}{c} \right)^i \frac{\delta P}{Pc} . \tag{4.2}$$

In addition to pressure, the magnetic field strength is required to calculate the TE polarization. The instrumental uncertainty in the magnetic field strength is $\delta B \sim 0.0032\%$. This value represents the uncertainty in magnetic field strength through the target cell based on predicted current settings and adjustments required. Though quite small, this value is not negligible in its effect on polarization. This error is used in the full error propagation of the TE polarization. Each component of statistical and fit uncertainty as well as the measurements instrumental uncertainty are added together. The final value of TE polarization uncertainty is calculated using the following expression,

$$\delta P_{TE} = \left( \left[ 1 - \tanh^2 \left( \frac{\mu B}{KT} \right) \frac{\mu}{KT} \delta T \right]^2 + \left[ \left( \tanh^2 \left( \frac{\mu B}{KT} \right) - 1 \right) \frac{\mu B}{KT^2} \delta B \right]^2 \right)^{1/2} . \tag{4.3}$$

The measurement's instrumental uncertainties are added into the error bar for that particular point. The total uncertainty is reduced in the fit over a set of measured pressures and areas, see Section 4.3. Because these measurement instrumental uncertainties are reduced in the fit they are not used as part of the system instrumental uncertainties listed in the next section (see Section 4.2). Instead a composite systematic component is listed as $\Delta T$.

| (#) | source | error (%) |
|---|---|---|
| (1) | $\Delta T$ | 1.45 |
| (2) | $\Delta A_{TE}$ | 1.61 |
| (3) | $\Delta A_{fit}$ | 0.75 |
| (4) | $R_B$ | 0.50 |
| (5) | $\Delta V_Q$ | 0.75 |
| (6) | NMR-tune | 0.47 |
| (7) | $\Delta V_{Yale}$ | 0.1 |
| (8) | $\Delta B_{drift}$ | 0.25 |
| (9) | $\Delta P_{run}$ | 0.53 |
| | $\Delta P/P$ | 2.58 |

**Table 1.** The system instrumental errors of the polarization measurement for protons in ammonia using DNP.

### 4.2 System Instrumental Uncertainty

It is necessary to consider several instrumental uncertainties that effect the quality of the polarization. In general, the NMR Q-circuit is susceptible to changes over time such as changes in coil material coupling effected by instability of field, coil orientation, vibration, and chemical changes as a function of dose. All of these type of contributions are expected to be negligible and can only be seen over multiple TE measurements. The major contributions to the uncertainty in the evaluation of the calibration constant were the uncertainty in the TE signal area at constant temperature and in the temperature $\Delta T$ of the material while taking the TE signal based on instrumental limitations. Because the uncertainty in temperature was used to weigh each point in a $\chi^2$-minimization fit, discussed in the next section, the uncertainty listed as $\Delta T$ is the residual error effect on polarization. The determination of the TE signal area has errors associated with it from the Riemann sum $\Delta A_{TE}$ and the Baseline fit $\Delta A_{fit}$. Another component of polarization uncertainty was the nonlinearities of the Q-meter circuit and changes in the electronic length of the $\Lambda/2$-cable as a function of temperature of the circuit itself denoted as $\Delta V_Q$. Additional main sources of uncertainty were tuning changes due to magnetoresistance of the coils and cables inside the cryostat, $R_B$, [11]. It is worth noting that using a cold NMR can greatly reduce the uncertainty associated with the NMR tune, see ref. [12].

Also considered are the shifts in NMR tune during data taking, the uncertainty in the gain voltage $\Delta V_{Yale}$, and the effect of the magnetic field drift during an experimental run $\Delta B_{drift}$. The uncertainty that comes from averaging over a run $\Delta P_{run}$ is discussed in Section 7. All components of uncertainty are listed in Table 1. The uncertainty $\Delta P_{run}$ is not instrumental but is listed as part of the total.

The total uncertainty found in polarization is 2.58%. This uncertainty is prior to the systematics involved in using the data to find the optimal calibration constant as well as the systematics involved in dealing with multiple TE measurements for the same consecutive usage of target material.

### 4.3 TE Fitting Algorithm

A systematic procedure that extracts the most information from the data was established to obtain each calibration constant for a given time period. An algorithm was developed specifically to investigate the area and pressure data taken during a TE and determine whether the TE was usable and which points should be in the fit to obtain the optimal area with respect to pressure and vice versa.

At thermal equilibrium, the pressure measurement should indicate only small thermal fluctuations outside the instrumental resolution of the device. Both the area and pressure should be flat over the series of points used in the TE measurement. It was possible to quantize the allowance of thermal fluctuation and dismiss data that has not had an appropriate relaxation time or not reached equilibrium. This was done using a two parameter line fit to study the slope of the line coming in and going out of the flattest range in the localized set of data points in which a TE has been taken. A limit can then be defined to be within a safe bound and flagged as *usable*. This quantization can then be use to judge the quality of TE data.

The procedure checks over the full range of the TE area and pressure measurements selecting the data with the smallest slope over the largest set of points. The criteria for being usable was a requirement of at least six points in area (pressure) spanning over the same time range in which a fit to a two parameter line returns a slope less than 0.0035 area/min (Torr/min). If this condition was met, the TE was classified a usable. All fits require the same degrees of freedom and same time range in the area and pressure. The starting points are a contiguous collection of six with the smallest slope from the two parameter line fit in the TE data. The number of contiguous points in the final one parameter line fit are increased until the two parameter line fit slope condition was no longer met or the uncertainty in the one parameter line fit increases with the addition rather than decreases. Points are increased one at a time, alternating from right to left under the give constraints. The one parameter line fit is then used to obtain the final area and pressure and associated uncertainties in these values. Fit examples of both the one and two parameter line fits are shown in Figure 5. The error bar associated with each point in the fit are the corresponding composite of statistical and systematic in which the instrumental is dominant in both cases. The fit results from pressure are transformed to temperature to find the $P_{TE}$. The uncertainty from pressure is used in Eq. 4.2 which is then used in Eq. 4.3. The area and uncertainty from the fit is then used to obtain the final calibration constant and associated uncertainty.

In the procedure described, the same maximal slope limit is used in both pressure and area, which is reasonable at thermal equilibrium. Area and pressure can both approach thermal equilibrium from vastly different trends depending on the initial conditions and state of the cryostat. An alternative usability criterion that is more sensitive to separate changes in area and pressure would be to use a limit based on relative percentage of the quantities in the fit. Using 0.2% of the one parameter line fit result leads to the same TE usability set as the mentioned fix slope limit. However, this method proves to be much more useful in testing the changes in area and pressure slightly before or after actual thermal equilibrium.

Finally, if there are multiple TE measurements taken over the same consecutive usage of material, the set of calibration constants are used in a one parameter line fit. Each TE must pass the criteria for being usable. The final fit was performed using a $\chi^2$-minimization weighting each cali-

bration in the fit by its combined total uncertainty. The minimized uncertainty from the fit was then used as the final error for that calibration constant.

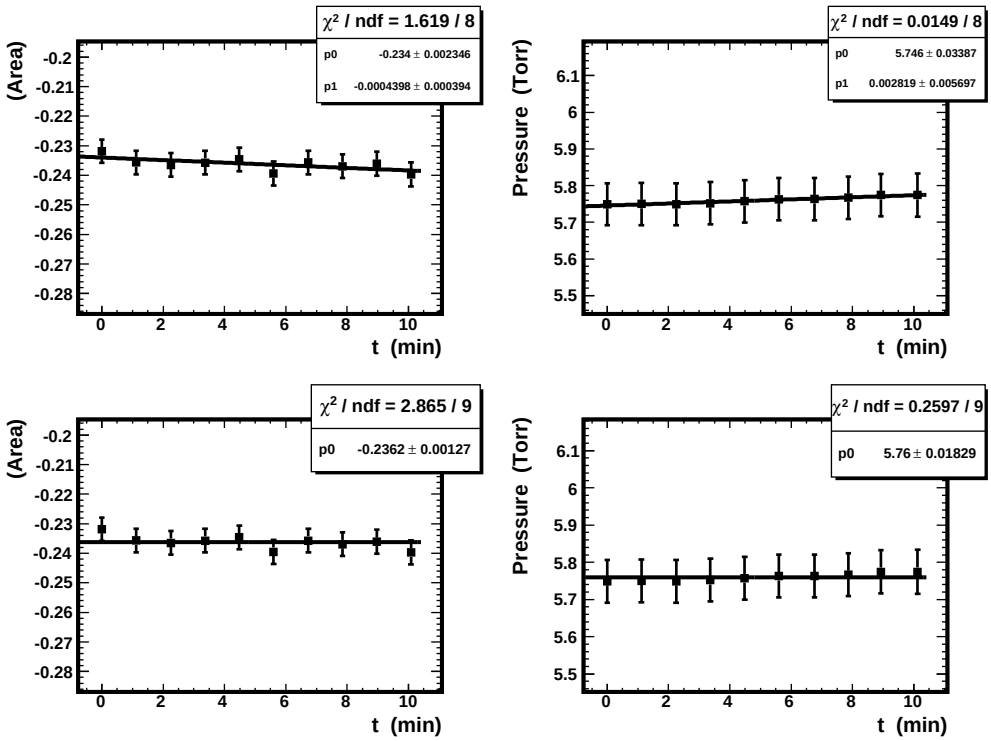


**Figure 5.** Example of fits in area and pressure analysis for TE. The top left (right) show the two parameter check on the slope of the line for area (pressure). The bottom left (right) show the final one parameter fit to a straight line for area (pressure).

## 5. Uncertainty Minimization

The cumulative uncertainty in the calibration constant represents the total systematic and statistical error. No other components of uncertainty go into the final polarization error implying that multiple TE measurements on consecutively used material with undisturbed target should fluctuate only in the scope of the cumulative uncertainties previously outlined. In this case, multiple TE measurements allow the reduction of the overall uncertainty by using a linear hypothesis which uses more information to obtain an optimal calibration constant.

However, it is also possible that the TE measurement was not good according to the algorithm's criteria or that a larger systematic change has occurred. Such changes include displacement of the NMR coil, large shifts in target material (target coil coupling changes), or large NMR tune changes which are all possible over the course of an experiment. If determined that such an effect has occurred and can be seen in the resulting calibration constant then the uncertainty must include the new systematic effect over that set of runs. Fortunately there is no indication of this in E08-007 the data.

**Table 2.** The date in which the target material was installed and then removed is listed along with the electron beam energy, label for top (T) or bottom (B) cup, the final calculated calibration constant, whether the TE was flagged as usable or not, and finally the TE start time from the experimental record used to find the TE data.

| Date | $E_{Beam}$ | Cup | $C_{TE}$ | Usable | TE start |
|---|---|---|---|---|---|
| 3/10-3/12 | 2.2 GeV | T | -1.299 (3.05%) | yes | 3-10 16:21:50 |
| | | | -1.422 (2.97%) | no | 3-12 16:42:00 |
| 3/10-3/12 | 2.2 GeV | B | -1.349 (3.06%) | yes | 3-10 16:56:55 |
| | | | -1.477 (6.20%) | yes | 3-12 17:30:20 |
| 4/17-4/19 | 1.7 GeV | B | -2.724 (3.02%) | no | 4-17 09:08:20 |
| | | | -1.823 (3.01%) | yes | 4-17 17:36:05 |
| 4/17-4/19 | 1.7 GeV | T | -3.020 (3.58%) | no | 4-26 13:10:00 |
| | | | -1.424 (2.94%) | yes | 4-30 01:30:25 |
| 4/30-5/5 | 1.1 GeV | B | -3.711 (3.12%) | no | 4-26 13:40:25 |
| | | | -1.799 (3.28%) | yes | 4-30 03:00:35 |
| 4/30-5/5 | 1.1 GeV | B | -1.731 (3.18%) | yes | 5-2 20:30:00 |

## 6. Final Systematics

Table 2 shows a summary of the calibration constants and uncertainties used over experiment E08-007. For each of the following a 5.0 T field at 6° target rotation was used. The Cup column indicates the results for the top (T) or bottom (B) target cups if both where used during the experiment. Some of the TE measurements were not used due to poor quality TE conditions. The TE measurements were flagged according to the algorithms criteria indicated in the Usable column. Also listed is the TE start time which was used to locate the TE in the polarization data. For configurations with multiple TE data, a final fit is used to produce the result used. From Table 2 one can see that there is only one set of TE measurements where both have been flagged as good. The final fit using -1.477 (6.20%) and -1.349 (3.06%) leads to a calibration constant of -1.371 (2.79%).

A summary of calibration constants and uncertainties over the sets of E08-007 runs are listed in Table 3. Both right and left arm data acquisition runs are listed along with the appropriate cup used for that set of runs. For production data, the final relative uncertainty in polarization for the experiment is less than or equal to 3.28%.

## 7. Polarization Data

Once the calibration constant is achieved along with the enhanced NMR signal integration, the Yale card gains and uncertainties, it is possible to calculate the final polarization which can be used in experimental analysis.

Each target event is stamped with time but to be useful each target event must be associated with a particular data acquisition run which recorded the physics data. All the events written to the target data files are broken down and configured into runs based on the run start and stop time. The

**Table 3.** The relative uncertainty over applied experimental run range with respect to the data taken on the left or right arm, with the top or bottom cups over the all runs for experiment E08-007.

| Run Range | Arm | Cup | $C_{TE}$ |
|---|---|---|---|
| 3061-3070 | Left | T | -1.299 (3.05%) |
| 3071-3084 | Left | B | -1.371 (2.79%) |
| 3085-3130 | Left | T | -1.299 (3.05%) |
| 4599-4695 | Left | B | -1.823 (3.01%) |
| 5339-5344 | Left | T | -1.424 (2.87%) |
| 5345-5346 | Left | B | -1.799 (3.28%) |
| 5347-5484 | Left | B | -1.731 (3.18%) |
| 22146-22155 | Right | T | -1.299 (3.05%) |
| 22156-22172 | Right | B | -1.371 (2.79%) |
| 22173-22217 | Right | T | -1.299 (3.05%) |
| 23540-23618 | Right | B | -1.823 (3.01%) |
| 24113-24118 | Right | T | -1.424 (2.87%) |
| 24120-24121 | Right | B | -1.799 (3.28%) |
| 24122-24258 | Right | B | -1.731 (3.18%) |

polarizations measured over time are charge averaged using the charge accumulated on the target material, see Fig. 1. The BCM currents are averaged over time between target events leading to a current which can be associated with a polarization for a given duration. The BCM currents are then used to calculate the charge accumulated on the target material for that run and charge average the polarizations. The charge average polarization for each run is what is required for physics analysis.

Because a charge average is used it is necessary to study the average deviation of polarization per run. This was obtained by studying runs in which the polarization naturally decays over time without sudden changes other than beam trips. A average deviation of 0.53% is found over the course of a standard run.

The final results are listed in Table 8.

## 8. Conclusion and Further Reduction

The uncertainties introduced by TE area $\Delta A_{TE}$, baseline fit $\Delta A_{fit}$, Q-meter $\Delta Q_T$, Yale card $\Delta V_{Yale}$, magnetic field variation $\Delta B_{drift}$, and variation in polarization over a run $\Delta P_{run}$ all have additional dependence that make the uncertainty change over the course of the experiment. Some of the dependence are simply changing conditions in the experiment and some change as a function of polarization. In the present results the uncertainty in each cases is overestimated based on extremal conditions throughout the entire experiment. Further uncertainty reduction can be made by implementing a run dependence to each of the listed components of uncertainty. Because these uncertainties are small even in the overestimation, an additional run dependence will not have a large effect.

For future experiments there are several key points that can be used to keep the acquired error to a minimum. Its possible to reduce the uncertainties introduced by TE area $\Delta A_{TE}$, and baseline fit $\Delta A_{fit}$ by making sure the TE peak is centered with a good baseline taken with at least three thousand sweeps. If the Q-meter temperature is regulated with a chiller, the deviation in temperature is reduced as is $\Delta Q_T$. Checking the position of the NMR signal frequently can reduce the effects of the uncertainty in magnetic field variation $\Delta B_{drift}$. Checking the stability of the NMR signal during Hall access and after the NMR tune can reduce unexpected changes once the experimental Hall goes to beam permit.

The value of $\Delta T$ is the uncertainty seen in the calibration constant based on the largest deviations seen in temperature combined with the largest deviation seen in TE area. This value could also be reduced by using the true deviation for that fit rather than the largest deviation seen. Ultimately this can make a difference when there are multiple TE measurements that will be used in a fit. It is essential to have the error bar of each point in the fit represented accurately so that each point is weighted correctly.

The largest reduction of uncertainty comes from having multiple TE measurements over the same consecutive use of a target material and using a $\chi^2$-minimization with a one parameter line hypothesis to fit the multiple calibration constants. The more quality TE measurements that are take the more the uncertainty can be reduced. Many TE measurements in the present study did not pass the constraints in the algorithm. This implies that the measurements where taken when the system did not fully reach thermal equilibrium or that enough points were not recorded once thermal equilibrium was reached.

During experiments, time is always an issue but considering the impact on uncertainty, it is far more valuable to skip taking the TE measurements when enough time will not be available to wait for true equilibrium and save the time to invest in getting more quality TE measurements for the essential data runs.

## References


[1] J. Arrington, D. Day, R. Gilman, D. Higinbotham, G. Ron, and A. Sarty, E08-007:*The proton form factor ratio at low $Q^2$* (2008), Jefferson Lab PR-08-007.

[2] D.G. Crabb, D.B. Day, Nucl. Instr. and Meth. in Phys. Res. A356, 9 (1995)

[3] Althoff KH, et al. Proc. 4th Wkshp Polar. Target Mat.Tech., ed. W Meyer, p. 23. Bonn: University of Bonn (1984)

[4] D.G. Crabb, Proc. 9th Int. Symp. High-Energy Spin Phys., Vol. 2:289, eds. W. Meyer, E. Steffens Thiel. Germany: Springer Verlag (1991)

[5] T.O. Niinikoski, J.M. Rieubland. Phys. Lett. 72A:141 (1979)

[6] D.A. Hill, J.J Hill. Argonne Natl. Lab. Rep. ANL-HEP-PR-81-05 (1981)

[7] L.G. DeMarco, A.S. Brill, D.G. Crabb, J. Chem. Phys., 108, 1423 (1998)

[8] J.C. Denard, A. Saha, *High Accuracy Beam Current Monitor System For CEBAF Experimental Hall A* (2001), Jefferson Lab Note: ACT01-12.

[9] G.R. Court, et al. Nucl. Instr. and Meth. A324:433 (1993)

[10] O. Kahn, Molecular Magnetism; VCH: New York, (1993)

[11] D. Kramer, Nucl. Instr. and Meth. in Phys. Res. A 356 (1995) 79-82

[12] G.R. Court, et al. Nucl. Instr. and Meth. in Phys. Res. A 527, 253 (2004)

**Table 4.** Final polarization data for experimental runs for E08-007. The experimental run with averaged polarization and uncertainty are given.

| Run | Polarization | Uncertainty |
|---|---|---|
| 3062 | 63.60534 | ± 1.93715 |
| 3063 | 53.22880 | ± 1.62112 |
| 3064 | 60.67218 | ± 1.84781 |
| 3065 | 42.50444 | ± 1.29450 |
| 3066 | 57.86787 | ± 1.76241 |
| 3067 | 57.49700 | ± 1.75111 |
| 3068 | 57.14256 | ± 1.74032 |
| 3069 | 55.87767 | ± 1.70179 |
| 3070 | 55.04434 | ± 1.67641 |
| 3071 | -54.59291 | ± 1.52543 |
| 3072 | -52.28429 | ± 1.46092 |
| 3073 | -50.29280 | ± 1.40528 |
| 3074 | -46.63690 | ± 1.30312 |
| 3075 | -43.22487 | ± 1.20778 |
| 3076 | -41.32180 | ± 1.15461 |
| 3077 | -47.37637 | ± 1.32379 |
| 3078 | -49.60276 | ± 1.38600 |
| 3079 | -50.72260 | ± 1.41729 |
| 3080 | -52.46336 | ± 1.46593 |
| 3081 | -52.91264 | ± 1.47848 |
| 3082 | -53.20552 | ± 1.48666 |
| 3083 | -53.10577 | ± 1.48388 |
| 3084 | -53.27825 | ± 1.48870 |
| 3085 | -87.49744 | ± 2.66480 |
| 4620 | 44.85352 | ±1.34942 |
| 4621 | 80.11055 | ±2.41013 |
| 4622 | 84.71269 | ±2.54859 |
| 4625 | 88.07842 | ± 2.64985 |
| 4626 | 88.02303 | ± 2.64818 |
| 4627 | 87.91672 | ± 2.64498 |
| 4628 | 87.16096 | ± 2.62225 |
| 4629 | 87.62569 | ± 2.63623 |
| 4630 | 87.55261 | ± 2.63403 |
| 4631 | 87.55125 | ± 2.63399 |
| 4632 | 87.72078 | ± 2.63909 |
| 4633 | 87.45707 | ± 2.63115 |
| 4634 | 87.40428 | ± 2.62957 |
| 4635 | 87.26829 | ± 2.62548 |
| 4636 | 87.25744 | ± 2.62515 |
| 4637 | 87.20536 | ± 2.62358 |
| 4638 | 87.02924 | ± 2.61828 |
| 4639 | 87.25762 | ± 2.62515 |
| 4640 | 87.02426 | ± 2.61813 |
| 4641 | 86.90623 | ± 2.61458 |
| 4642 | 86.85336 | ± 2.61299 |
| 4643 | 86.63011 | ± 2.60628 |

| Run | Polarization | Uncertainty |
|---|---|---|
| 4644 | 86.57609 | ± 2.60465 |
| 4645 | 86.42974 | ± 2.60025 |
| 4646 | 86.55712 | ± 2.60408 |
| 4647 | 87.67862 | ± 2.63782 |
| 4648 | 87.19927 | ± 2.62340 |
| 4649 | 86.92172 | ± 2.61505 |
| 4650 | 86.92845 | ± 2.61525 |
| 4651 | 58.01461 | ± 1.74538 |
| 4652 | 86.74981 | ± 2.60988 |
| 4653 | 86.49934 | ± 2.60234 |
| 4654 | 86.30430 | ± 2.59647 |
| 4655 | 85.04596 | ± 2.55862 |
| 4656 | -74.70928 | ± 2.24764 |
| 4659 | -77.99493 | ± 2.34649 |
| 4660 | -78.86586 | ± 2.37269 |
| 4661 | -79.66590 | ± 2.39676 |
| 4662 | -79.87363 | ± 2.40301 |
| 4663 | -80.34520 | ± 2.41719 |
| 4664 | -80.76485 | ± 2.42982 |
| 4665 | -80.97010 | ± 2.43599 |
| 4666 | -81.13207 | ± 2.44087 |
| 4667 | -81.12083 | ± 2.44053 |
| 4668 | -81.38196 | ± 2.44838 |
| 4669 | -81.32940 | ± 2.44680 |
| 4670 | -80.92299 | ± 2.43458 |
| 4671 | -80.72273 | ± 2.42855 |
| 4672 | -81.29049 | ± 2.44563 |
| 4673 | -81.13855 | ± 2.44106 |
| 4674 | -81.65337 | ± 2.45655 |
| 4675 | -81.40888 | ± 2.44919 |
| 4676 | -81.38903 | ± 2.44860 |
| 4677 | -81.27798 | ± 2.44526 |
| 4678 | -81.05349 | ± 2.43850 |
| 4679 | -80.93738 | ± 2.43501 |
| 4680 | -81.31865 | ± 2.44648 |
| 4681 | -80.88878 | ± 2.43355 |
| 4682 | -81.11262 | ± 2.44028 |
| 4683 | -80.65619 | ± 2.42655 |
| 4684 | -80.84912 | ± 2.43235 |
| 4685 | -80.83289 | ± 2.43187 |
| 4686 | -80.87981 | ± 2.43328 |
| 4687 | -80.72890 | ± 2.42874 |
| 4688 | -80.36132 | ± 2.41768 |
| 4689 | -81.41964 | ± 2.44952 |
| 4690 | -81.17599 | ± 2.44219 |
| 4691 | -80.99016 | ± 2.43659 |
| 4692 | -80.89385 | ± 2.43370 |
| 4693 | -80.99735 | ± 2.43681 |
| 5346 | 74.40601 | ± 2.36801 |

| | | |
|---|---|---|
| 5347 | 80.88591 | ± 2.57423 |
| 5348 | 81.28951 | ± 2.58708 |
| 5349 | 81.41773 | ± 2.59116 |
| 5350 | 81.76495 | ± 2.60221 |
| 5351 | 81.91310 | ± 2.60693 |
| 5352 | 82.03371 | ± 2.61076 |
| 5353 | 82.33157 | ± 2.62024 |
| 5354 | 82.25681 | ± 2.61786 |
| 5355 | 82.36064 | ± 2.62117 |
| 5356 | 82.40491 | ± 2.62258 |
| 5357 | 82.37593 | ± 2.62166 |
| 5358 | 82.37247 | ± 2.62155 |
| 5359 | 82.38672 | ± 2.62200 |
| 5360 | 82.33959 | ± 2.62050 |
| 5361 | 82.55797 | ± 2.62745 |
| 5362 | 82.43962 | ± 2.62368 |
| 5363 | 82.57619 | ± 2.62803 |
| 5364 | 82.40893 | ± 2.62271 |
| 5365 | 82.31965 | ± 2.61986 |
| 5366 | 82.23339 | ± 2.61712 |
| 5367 | 82.18284 | ± 2.61551 |
| 5368 | 82.21743 | ± 2.61661 |
| 5369 | 82.09092 | ± 2.61258 |
| 5370 | 82.11409 | ± 2.61332 |
| 5371 | 82.01505 | ± 2.61017 |
| 5372 | 82.15581 | ± 2.61465 |
| 5373 | 81.72989 | ± 2.60109 |
| 5374 | 81.82677 | ± 2.60418 |
| 5375 | 83.67144 | ± 2.66289 |
| 5376 | 83.50354 | ± 2.65754 |
| 5377 | 83.60015 | ± 2.66062 |
| 5378 | 83.15945 | ± 2.64659 |
| 5379 | 83.07526 | ± 2.64391 |
| 5380 | 82.47581 | ± 2.62483 |
| 5381 | 82.52591 | ± 2.62643 |
| 5382 | 82.44314 | ± 2.62379 |
| 5383 | 82.21340 | ± 2.61648 |
| 5384 | 82.46205 | ± 2.62440 |
| 5385 | 82.40611 | ± 2.62262 |
| 5386 | 82.34884 | ± 2.62079 |
| 5387 | 82.09455 | ± 2.61270 |
| 5388 | 81.60317 | ± 2.59706 |
| 5389 | 81.97681 | ± 2.60895 |
| 5390 | -76.28099 | ± 2.42768 |
| 5391 | -77.61975 | ± 2.47029 |
| 5393 | -78.24254 | ± 2.49011 |
| 5394 | -78.55518 | ± 2.50008 |
| 5395 | -78.49186 | ± 2.49804 |
| 5396 | -78.51029 | ± 2.49863 |

| | | |
|---|---|---|
| 5397 | -78.34060 | ± 2.49323 |
| 5398 | -78.40358 | ± 2.49523 |
| 5399 | -78.13085 | ± 2.48655 |
| 5400 | -79.26247 | ± 2.52257 |
| 5401 | -78.49695 | ± 2.49820 |
| 5402 | -79.14350 | ± 2.51878 |
| 5403 | -79.11921 | ± 2.51801 |
| 5404 | -78.81400 | ± 2.50830 |
| 5405 | -78.82597 | ± 2.50868 |
| 5406 | -78.90935 | ± 2.51133 |
| 5407 | -78.67926 | ± 2.50401 |
| 5408 | -78.65667 | ± 2.50329 |
| 5409 | -78.74458 | ± 2.50609 |
| 5410 | -78.22288 | ± 2.48948 |
| 5413 | -79.31243 | ± 2.52416 |
| 5414 | -79.22584 | ± 2.52140 |
| 5415 | -79.23806 | ± 2.52179 |
| 5416 | -79.21270 | ± 2.52098 |
| 5417 | -79.10288 | ± 2.51749 |
| 5418 | -79.27653 | ± 2.52302 |
| 5419 | -79.14579 | ± 2.51885 |
| 5420 | -79.05783 | ± 2.51605 |
| 5421 | -79.19667 | ± 2.52047 |
| 5422 | -79.19205 | ± 2.52033 |
| 5423 | -79.24529 | ± 2.52202 |
| 5424 | -79.15489 | ± 2.51914 |
| 5425 | -78.98742 | ± 2.51381 |
| 5426 | -78.80072 | ± 2.50787 |
| 5427 | -78.80202 | ± 2.50791 |
| 5428 | -78.70492 | ± 2.50482 |
| 5429 | -78.50912 | ± 2.49859 |
| 5430 | -78.33983 | ± 2.49320 |
| 5431 | -78.28605 | ± 2.49149 |
| 5432 | -78.57889 | ± 2.50081 |
| 5433 | -78.83175 | ± 2.50886 |
| 5434 | -78.44354 | ± 2.49650 |
| 5435 | -78.33056 | ± 2.49291 |
| 5436 | -78.24394 | ± 2.49015 |
| 5437 | -78.33703 | ± 2.49312 |
| 5438 | -78.25868 | ± 2.49062 |
| 5439 | -78.16636 | ± 2.48768 |
| 5440 | -78.13838 | ± 2.48679 |